

Models for Arginine–Metal Binding. Synthesis of Guanidine and Urea Ligands through Amination and Hydration of a Cyanamide Ligand Bound to Platinum(II), Osmium(III), and Cobalt(III)

David P. Fairlie,^{*,†,‡} W. Gregory Jackson,[§] Brian W. Skelton,^{||} Huo Wen,^{||} Allan H. White,^{||} Wasantha A. Wickramasinghe,[†] Tai Chin Woon,[†] and Henry Taube[‡]

The 3D Centre, University of Queensland, Brisbane, Qld 4072, Australia; Department of Chemistry, Stanford University, Stanford, California 94305-5080; Department of Chemistry, University College (NSW), Australian Defence Force Academy, Canberra, ACT 2600, Australia; and Department of Chemistry, University of Western Australia, Perth, WA 6907, Australia

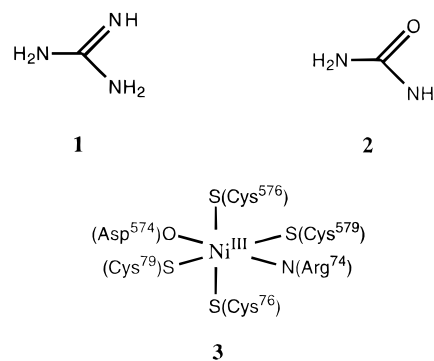
Received September 13, 1996[⊗]

Dimethylcyanamide ($\text{N}\equiv\text{CNMe}_2$) has been coordinated to both hard and soft electrophiles ($(\text{NH}_3)_5\text{Co}^{3+}$, $(\text{NH}_3)_5\text{Os}^{3+}$, $(\text{dien})\text{Pt}^{2+}$) which activate ($\sim\times 10^6$) the nitrile toward attack by nucleophiles such as ammonia and hydroxide. *Amination* with liquid ammonia gave a rare coordinated guanidine (*N,N*-dimethylguanidine) ligand, which NMR spectra and X-ray crystal structures show to be charge neutral rather than anionic. Crystals of $[(\text{NH}_3)_5\text{CoNH}=\text{C}(\text{NH}_2)\text{NMe}_2](\text{S}_2\text{O}_6)_{3/2}\cdot\text{H}_2\text{O}$, $\text{CoC}_3\text{H}_{26}\text{N}_8\text{O}_{10}\text{S}_3$, were triclinic, space group $P\bar{1}$, $a = 11.565(2)$ Å, $b = 10.629(5)$ Å, $c = 8.026(1)$ Å, $\alpha = 84.93(3)^\circ$, $\beta = 76.01(1)^\circ$, $\gamma = 73.82(3)^\circ$, $V = 919.2(5)$ Å³, $Z = 2$, and R_F (R_{wF}) = 0.038 (0.047) for 3262 observed reflections ($I > 3.0 \sigma(I)$). Crystals of $[(\text{dien})\text{PtNH}=\text{C}(\text{NH}_2)\text{NMe}_2](\text{CF}_3\text{SO}_3)_2$, $\text{PtC}_9\text{H}_{22}\text{N}_6\text{O}_6\text{S}_2\text{F}_6$, are monoclinic, space group $P2_1/c$, $a = 13.857(4)$, $b = 14.748(4)$ Å, $c = 22.092(4)$ Å, $\beta = 105.38(2)^\circ$, $V = 4353(2)$ Å³, $Z = 8$, and R_F (R_{wF}) = 0.034 (0.038) for 6778 reflections. Coordination geometries around the metals are octahedral and square planar, respectively, the guanidine skeletons being planar with bond angles and lengths characteristic of the metal–imino (rather than metal–amino) tautomer. The complexes are very stable in coordinating solvents (DMSO; water, pH 3–11) indicating high affinity of guanidine ligands for metal ions. *Hydration* of the dimethylcyanamide ligand is base-catalyzed, and first-order in $[\text{OH}^-]$ (0.05–0.5 M NaOH; $k = k_s + k_{\text{OH}}[\text{OH}^-]$, $k_{\text{OH}} = 2\text{--}5 \text{ M}^{-1} \text{ s}^{-1}$, 25 °C), in each case producing coordinated *N,N*-dimethylurea ($[(\text{dien})\text{PtNHCONMe}_2]^+$, $[(\text{NH}_3)_5\text{CoNHCONMe}_2]^{2+}$, $[(\text{NH}_3)_5\text{OsNHCONMe}_2]^{2+}$). Hydration rates are surprisingly similar despite differing radial extensions of the metal d-orbitals, a finding consistent with their comparable polarizing powers but contrary to expectation from other work. The relevance of metal activation of nitriles to biological systems is discussed.

Introduction

Guanidine (**1**), unlike the isoelectronic molecule urea (**2**), is presently unknown as a ligand for biological metal ions despite its presence in arginine which is frequently found in active sites of enzymes. In water guanidine is protonated ($\text{p}K_a \sim 12.5$) but in hydrophobic environments created by folded proteins, alternative electrophiles like metal ions may compete better with the proton for **1**. For example the guanidine of Arg-74 in (NiFe)hydrogenase (*D. gigas*) has been proposed¹ to be a critical ligand for the Ni(III) complex **3**.

X-ray crystal structures have been determined for only a few complexes bound to guanidine-like ligands,^{2–5} including bridg-



* Correspondence can be addressed to D.P.F. at the University of Queensland. E-mail: d.fairlie@mailbox.uq.oz.au. Fax: +61-7-33651990.

† University of Queensland.

‡ Stanford University.

§ University College (UNSW).

|| University of Western Australia.

⊗ Abstract published in *Advance ACS Abstracts*, February 15, 1997.

(1) Przybyla, A. E.; Robbins, J.; Menon, N.; Peck, H. D., Jr. *FEMS Microbiol. Rev.* **1992**, *88*, 109.

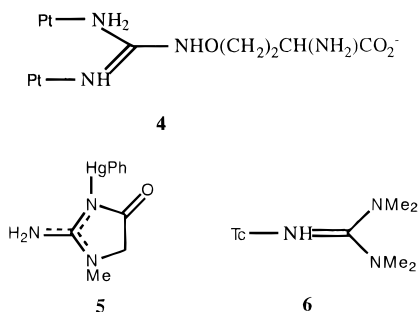
(2) (a) Ratilla, E. M. A.; Scott, B. K.; Moxness, M. S.; Kostic, N. M. *Inorg. Chem.* **1990**, *29*, 918. (b) Ratilla, E. M. A.; Kostic, N. M. *J. Am. Chem. Soc.* **1988**, *110*, 4427.

(3) (a) Canty, A. J.; Chaichit, N.; Gatehouse, B. M. *Acta Crystallogr.* **1979**, *B35*, 592. (b) Canty, A. J.; Fyfe, M.; Gatehouse, B. M. *Inorg. Chem.* **1978**, *17*, 1467.

(4) Vries, N.; Costello, C. E.; Jones, A. G.; Davison, A. *Inorg. Chem.* **1990**, *29*, 1348.

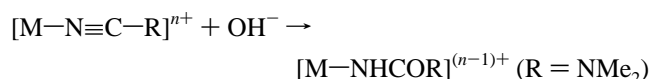
ing canavagine² (**4**), monodentate creatinine³ (**5**) and tetramethylguanidine⁴ (**6**) bound to two $\{(\text{terpy})\text{Pt}^{\text{II}}\}$, one Hg^{II} and a Te^{V} (nitride), respectively. Since most biologically relevant metal ions are substitution labile, we decided to use a series of kinetically more inert metal centers of varying “hardness” in an attempt to trap a basic guanidine molecule as a ligand. We now report the synthesis and characterization of *monodentate* 1,1-dimethylguanidine ($\text{NH}=\text{C}(\text{NH}_2)\text{NMe}_2$) complexes of hard $(\text{NH}_3)_5\text{Co}^{\text{III}}$, soft $(\text{dien})\text{Pt}^{\text{II}}$, and intermediate⁶ $(\text{NH}_3)_5\text{Os}^{\text{III}}$, includ-

(5) (a) Sulfaguandine: Alleaume, M.; Gulko, A.; Herstein, F. H.; Kapon, M.; Marsh, R. E. *Acta Crystallogr.* **1976**, *B32*, 669. (b) Cimetidine: Soto, L.; Legros, J. P.; Sancho, A. *Polyhedron* **1988**, *7*, 307. (c) Cyanoguanidine: Begley, M. J.; Hubberstey, P.; Walton, P. H. *J. Chem. Soc., Chem. Commun.* **1989**, 502.



ing two of the first X-ray crystal structures of a metal-bonded guanidine residue. These complexes are kinetically very stable and could be useful models for Arg bound to more labile metal ions in biological systems.

Our synthetic route to guanidine complexes relies upon the electrophilic activation of a nitrile ($\text{N}\equiv\text{CNMe}_2$) by a metal ion, a process implicated in biological systems for non-haem Fe(III).⁷ We therefore also briefly examined the degree of electrophilic activation of the nitrile ligand by metal ions (Pt(II), Os(III), and Co(III)) by measuring rates of base-catalyzed hydration of this cyanamide ligand to the corresponding urea ligand, known to coordinate to both hard and soft metal ions⁸ including Ni(II) in the enzyme urease.⁹



Previous work¹⁰ gave evidence that base-catalyzed hydration of acetonitrile ($\text{R} = \text{Me}$), coordinated to $(\text{NH}_3)_5\text{Co}^{\text{III}}$, $(\text{NH}_3)_5\text{-Rh}^{\text{III}}$, and $(\text{NH}_3)_5\text{Ir}^{\text{III}}$, was not first-order in $[\text{OH}^-]$ and suggested that greater d-orbital radii of the heavier metals influenced the hydration rate.¹⁰ We examine this hypothesis here under similarly limited conditions (0.05–0.5 M $[\text{OH}^-]$) for hydration of a cyanamide ligand on Co^{III} , Os^{III} , and Pt^{II} .

In the light of these results, roles for metal activation of nitriles in biological systems are briefly discussed.

Results and Discussion

Nitrile Complexes. Nitrile complexes were prepared by substituting nitrile solvent for the weakly held trifluoromethane-

Table 1. Comparison of Infrared Stretching Frequencies^a of Nitriles and Their Metal Complexes

	ν , cm^{-1}	ref
$\text{N}\equiv\text{CMe}$	2254 m	15d
$[(\text{NH}_3)_5\text{OsN}\equiv\text{CMe}](\text{CF}_3\text{SO}_3)_2$	2200 s	this work
$[(\text{NH}_3)_5\text{RuN}\equiv\text{CMe}](\text{BF}_4)_2$	2239 s	15e
$[(\text{NH}_3)_5\text{RhN}\equiv\text{CMe}](\text{ClO}_4)_3$	2323 w	15e
$[(\text{dien})\text{PtN}\equiv\text{CMe}](\text{CF}_3\text{SO}_3)_2$	2305 w	this work
$[(\text{NH}_3)_5\text{CoN}\equiv\text{CMe}](\text{CF}_3\text{SO}_3)_3$	2320 w	16g
$[(\text{NH}_3)_5\text{OsN}\equiv\text{CMe}](\text{CF}_3\text{SO}_3)_3$	2300 w	this work
$[(\text{NH}_3)_5\text{RuN}\equiv\text{CMe}](\text{ClO}_4)_3$	2286 m	15d
$\text{N}\equiv\text{CNMe}_2$	2217 s	this work
$[(\text{dien})\text{PtN}\equiv\text{CNMe}_2](\text{CF}_3\text{SO}_3)_2$	2297 s	this work
$[(\text{NH}_3)_5\text{CoN}\equiv\text{CNMe}_2]^{3+}$	2280 s	8b
$[(\text{NH}_3)_5\text{OsN}\equiv\text{CNMe}_2](\text{BF}_4)_3$	2250 s	this work
$[(\text{NH}_3)_5\text{RuN}\equiv\text{CNMe}_2](\text{CF}_3\text{SO}_3)_3$	2280 s	8f

^a Energy of IR stretches can vary substantially with anion. Abbreviations: s = strong; m = medium; w = weak.

sulfonate ligand^{11,12} of $[(\text{NH}_3)_5\text{Co}^{\text{III}}(\text{CF}_3\text{SO}_3)]^{3+}$ and $[(\text{NH}_3)_5\text{-Os}^{\text{III}}(\text{CF}_3\text{SO}_3)]^{3+}$ or the readily displaceable¹³ water ligand of $[\text{dienPtOH}_2](\text{CF}_3\text{SO}_3)_2$. Products were characterized by their infrared (Table 1) and, for the diamagnetic Pt^{II} and Co^{III} complexes, their NMR (^1H , ^{13}C) spectral data. The ^{13}C -NMR chemical shift for the sp-hybridized carbon of metal-coordinated dimethylcyanamide (120–130 ppm) was particularly diagnostic. The paramagnetic Os^{III} analogue was alternatively characterized (see Experimental Section) by its UV absorption and a unique band in the near-infrared region of the electromagnetic spectrum. These data support coordination to the metal via the nitrile rather than the amino nitrogen, but the observed enhanced reactivity (vide infra) of the nitrile toward nucleophilic attack is far more compelling evidence of the coordination mode. The equilibrium between linkage isomers thus lies to the left:



The infrared stretch for the nitrile of the coordinated dimethylcyanamide is typically more intense in all its complexes than for acetonitrile and other nitrile complexes.¹⁴ Also the infrared stretch (Table 1) for the cyanamide nitrile in $[\text{dienPtN}\equiv\text{CNMe}_2](\text{CF}_3\text{SO}_3)_2$, $[(\text{NH}_3)_5\text{OsN}\equiv\text{CNMe}_2](\text{BF}_4)_3$ and $[(\text{NH}_3)_5\text{CoN}\equiv\text{CNMe}_2](\text{CF}_3\text{SO}_3)_3$ was typically at higher energy (2250–2300 cm^{-1}) than for the uncoordinated cyanamide (2217 cm^{-1}), rather than the reverse trend when the metal has π -donor capacity and the nitrile acts as a π -acceptor (e.g. $\text{Ru}(\text{II})$ and $\text{Os}(\text{II})$, Table 1). We note that $(\text{NH}_3)_5\text{Os}(\text{III})$, which is thought to have some π -donor character,¹² exhibited a stretch at 2250–2300 cm^{-1} . The Os^{III} complex also gave an unusual band in the near-infrared region (see Experimental Section) of the

- (6) (a) Taube, H. *Pure Appl. Chem.* **1979**, *51*, 901. (b) Taube, H. *Coord. Chem. Rev.* **1978**, *26*, 33. (c) Taube, H. *Comments Inorg. Chem.* **1981**, *1*, 17.
- (7) (a) Nagasawa, T.; Yamada, H. *Biochem. Biophys. Res. Commun.* **1987**, *147*, 701. (b) Thompson, L. A.; Knowles, C. J.; Linton, E. A.; Wyatt, J. M. *Chem. Br.* **1988**, 900. (c) Hönicke-Schmidt, P.; Schneider, M. P. *J. Chem. Soc., Chem. Commun.* **1990**, 648. (d) Jin, H.; Turner, I. M.; Nelson, M. J.; Gubriel, R. J.; Doan, P. E.; Hoffman, B. M. *J. Am. Chem. Soc.* **1993**, *115*, 5290.
- (8) N-bonded ureas on Co(III): (a) Fairlie, D. P.; Jackson, W. G. *Inorg. Chim. Acta* **1988**, *150*, 81. (b) Dixon, A. M.; Fairlie, D. P.; Jackson, W. G.; Sargeson, A. M. *Inorg. Chem.* **1983**, *22*, 4038. On Rh(III): (c) Curtis, N. J.; Dixon, N. E.; Sargeson, A. M. *J. Am. Chem. Soc.* **1983**, *105*, 5347. On Ru(III): (d) Fairlie, D. P.; Taube, H. *Inorg. Chem.* **1985**, *24*, 3199. On Pt(II): (e) Woon, T. C.; Wickramasinghe, W. A.; Fairlie, D. P. *Inorg. Chem.* **1993**, *32*, 2190. On Os(III) and Ru(III): (f) Fairlie, D. P.; Taube, H. To be submitted for publication. On Cu(II) and Ni(II): (g) Maslak, P.; Sczepanski, J. L.; Parvez, M. *J. Am. Chem. Soc.* **1991**, *113*, 1062.
- (9) (a) Andrews, R. K.; Blakeley, R. L.; Zerner, B. In *The Bioinorganic Chemistry of Nickel*; Lancaster, J. R., Jr., Ed.; VCH Publishers: New York, 1988; p 141. (b) Hausinger, R. P. Biochemistry of Nickel. In *Biochemistry of the Elements*, Plenum Press: New York, 1993; Vol. 12, Chapter 3, p 23.
- (10) Curtis, N. J.; Sargeson, A. M. *J. Am. Chem. Soc.* **1984**, *106*, 625.

- (11) Dixon, N. E.; Jackson, W. G.; Lancaster, M. J.; Lawrance, G. A.; Sargeson, A. M. *Inorg. Chem.* **1981**, *20*, 470.
- (12) Lay, P. A.; Magnuson, R. H.; Taube, H. *J. Am. Chem. Soc.* **1982**, *104*, 7685.
- (13) Woon, T. C.; Fairlie, D. P. *Inorg. Chem.* **1992**, *31*, 4069.
- (14) Johnson, A.; Taube, H. *Indian J. Chem.* **1989**, *66*, 503.
- (15) (a) Zanella, A. W.; Ford, P. C. *Inorg. Chem.* **1975**, *14*, 42. (b) Zanella, A. W.; Ford, P. C. *Inorg. Chem.* **1975**, *14*, 700. (c) Zanella, A. W.; Ford, P. C. *J. Chem. Soc., Chem. Commun.* **1975**, 795. (d) Clarke, R. E.; Ford, P. C. *Inorg. Chem.* **1970**, *9*, 227. (e) Foust, R. D.; Ford, P. C. *Inorg. Chem.* **1972**, *11*, 899.
- (16) (a) Buckingham, D. A.; Keene, F. R.; Sargeson, A. M. *J. Am. Chem. Soc.* **1973**, *95*, 5649. (b) Butler, D. G.; Creaser, I. I.; Dyke, S. F.; Sargeson, A. M. *Acta Chem. Scand.*, A **1978**, *32*, 789. (c) Creaser, I. I.; Harrowfield, J. MacB.; Keene, F. R.; Sargeson, A. M. *J. Am. Chem. Soc.* **1981**, *103*, 3559. (d) Pinnell, D.; Wright, G. B.; Jordan, R. B. *J. Am. Chem. Soc.* **1972**, *94*, 6104. (e) Balahura, R. J.; Cock, P.; Purcell, W. L. *J. Am. Chem. Soc.* **1974**, *96*, 2739. (f) Balahura, R. J.; Purcell, W. L. *Inorg. Chem.* **1981**, *20*, 4159. (g) Jordan, R. B.; Sargeson, A. M.; Taube, H. *Inorg. Chem.* **1966**, *5*, 1091.

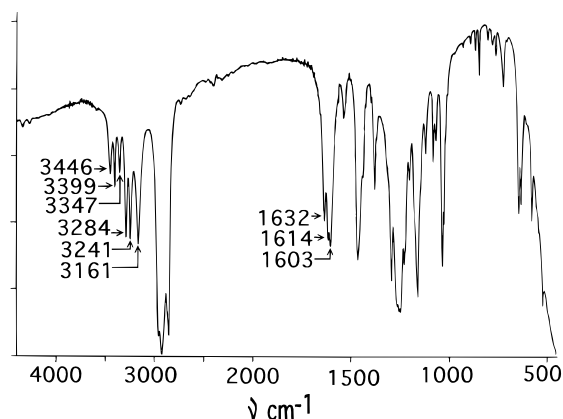
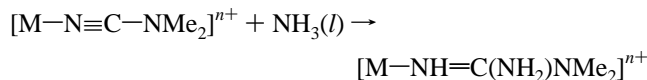


Figure 1. Infrared spectrum of $[\text{dienPtNH}=\text{C}(\text{NH}_2)\text{NMe}_2](\text{CF}_3\text{SO}_3)_2$ (KBr disk) for ν_{NH} and ν_{NH_2} regions.

electromagnetic spectrum which is characteristic of Os^{III} and has been attributed to spin orbital coupling.¹² Its intensity also appears^{8f} to be typical of aminonitriles bonded to $(\text{NH}_3)_5\text{Os}^{\text{III}}$ via a nitrile nitrogen and this assignment is supported by the electrophilic activation of the nitrile (see ahead).

Amination of the Nitrile. When neat $\text{NH}_3(l)$ was reacted with $[\text{dienPtN}\equiv\text{CNMe}_2](\text{CF}_3\text{SO}_3)_2$, $[(\text{NH}_3)_5\text{OsN}\equiv\text{CNMe}_2](\text{BF}_4)_3$ or $[(\text{NH}_3)_5\text{CoN}\equiv\text{CNMe}_2](\text{CF}_3\text{SO}_3)_3$, amination quantitatively produced the new guanidine complexes within minutes:



After evaporation of the $\text{NH}_3(l)$ and recrystallization from aqueous 0.1M Tris (pH 10), complexes contained uncharged rather than anionic guanidine ligands. This was established by elemental composition, and for $[\text{dienPtNH}=\text{C}(\text{NH}_2)\text{NMe}_2]^{2+}$ and $[(\text{NH}_3)_5\text{CoNH}=\text{C}(\text{NH}_2)\text{NMe}_2]^{3+}$ by ^1H NMR measurements in $\text{DMSO}-d_6$ since each complex displayed two guanidine NH resonances in the expected 2:1 ratio at ~ 6 ppm (NH_2) and ~ 2.5 – 4.5 ppm ($\text{M}-\text{NH}=\text{C}$). The chemical shift of the $\text{M}-\text{NH}=\text{C}$ proton was similar to that for the analogous proton in the isoelectronic amide complexes (e.g. $[\text{dienPtNH}=\text{C}(\text{OH})\text{R}]^{2+}$ or $[(\text{NH}_3)_5\text{CoNHC}(\text{OH})\text{R}]^{3+}$, $\text{R} = \text{Me}$ or H).^{13,17} The ^{13}C -NMR spectrum also showed the characteristic chemical shift for an sp^2 guanidine carbon (162 ppm, $\text{DMSO}-d_6$) for both complexes. The guanidine complexes are very stable in coordinating solvents (water, DMSO , NH_3), with no reactions detected over several weeks.

Both the solution data above and the solid state data below show that the guanidine ligand exists in the imino (**7**) rather than the amino (**8**, **9**) tautomeric form. Steric interactions with Me groups would presumably disfavor **9**. The infrared spectrum

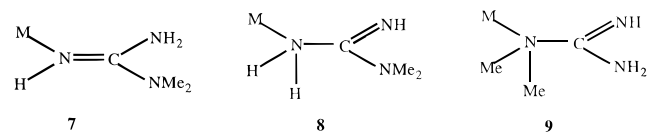


(Figure 1) is a particularly useful fingerprint for characterizing the platinum complex with three sharp peaks (1603, 1615, 1632 cm^{-1}) for the three C–N bonds as well as six sharp N–H stretches (~ 3100 – 3500 cm^{-1}). The three highest energy

(17) (a) Angel, R.; Fairlie, D. P.; Jackson, W. G. *Inorg. Chem.* **1990**, *29*, 20. (b) Fairlie, D. P.; Angus, P. M.; Fenn, M. D.; Jackson, W. G. *Inorg. Chem.* **1991**, *30*, 1564.

Table 2. Selected Crystallographic Data for $[(\text{NH}_3)_5\text{CoNH}=\text{C}(\text{NH}_2)\text{NMe}_2](\text{S}_2\text{O}_6)_3 \cdot 2\text{H}_2\text{O}$ (**10**) and $[\text{dienPtNH}=\text{C}(\text{NH}_2)\text{NMe}_2](\text{CF}_3\text{SO}_3)_2$ (**11**)

	10	11
formula	$\text{C}_6\text{H}_{52}\text{Co}_2\text{N}_{16}\text{O}_{26}\text{S}_6$	$\text{C}_9\text{H}_{22}\text{F}_6\text{N}_6\text{O}_6\text{PtS}_2$
M_r	978.8	683.5
cryst dimens, mm	$0.08 \times 0.15 \times 0.24$	$0.60 \times 0.62 \times 0.27$
cryst syst	triclinic	monoclinic
space group	$P\bar{1}$ (C_1^1 , No. 2)	$P2_1/c$ (C_{2h}^2 , No. 14)
a , Å	11.565(2)	13.857(4)
b , Å	10.629(5)	14.748(4)
c , Å	8.026(1)	22.092(4)
α , deg	84.93(3)	90
β , deg	76.01(1)	105.38(2)
γ , deg	73.82(3)	90
V , Å ³	919.2(5)	4353(2)
Z	1	8
ρ_{calc} , $\text{g}\cdot\text{cm}^{-3}$	1.77	2.09
F_{000}	510	2640
μ (Mo), cm^{-1}	12.6	67
A^* : min; max	1.10; 1.19	3.66; 13.2
R^a (R_w^b)	0.038 (0.047)	0.034 (0.038)
T (K)	~ 293	~ 293
λ (Mo), Å	0.7107 ₃	0.7107 ₃
$2\theta_{\text{max}}$ ($2\theta/\theta$ scan), deg	55	65
no. of reflns, indep	3952	15738
no. of reflns, obsd ^c	3262	6778 [$I > 3\sigma(I)$]
no. of params, refined	323	719

^a $R = \Sigma||F_o| - |F_c||/\Sigma|F_o|$. ^b $R_w = [\Sigma w(|F_o| - |F_c|)^2/\Sigma w|F_o|^2]^{1/2}$; statistical weights derivative of $\sigma^2(I) = \sigma^2(I_{\text{diff}}) + 0.0004\sigma^4(I_{\text{diff}})$. ^c Unique data to 65°; an additional hemisphere was measured to $2\theta_{\text{max}}$ 30° and merged to enhance the precision of the low-angle data to assist hydrogen atom definition.

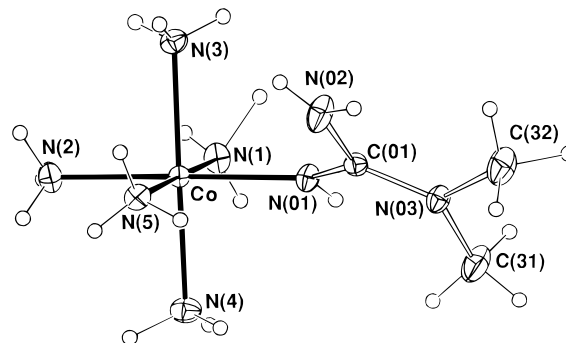


Figure 2. The cation of **10**. 20% thermal ellipsoids are shown for non-hydrogen atoms, hydrogens having arbitrary radii of 0.1 Å.

stretches are assigned to coordinated guanidine and the remainder to the dien ligand. The analogous pentaammineosmium(III) and pentaamminecobalt(III) complexes gave a broad unresolved signal in each wavelength range.

Guanidine Structures. Table 2 gives crystallographic details for the X-ray structures of **10**, $[(\text{NH}_3)_5\text{CoNH}=\text{C}(\text{NH}_2)\text{NMe}_2](\text{S}_2\text{O}_6)_{3/2} \cdot \text{H}_2\text{O}$, and **11**, $[\text{dienPtNH}=\text{C}(\text{NH}_2)\text{NMe}_2](\text{CF}_3\text{SO}_3)_2$. ORTEP drawings of the cation structures, with numbering schemes, are presented in Figures 2 and 3 respectively. The Co and Pt coordination geometries are the expected octahedral and square planar respectively, and the guanidine ligands are planar. Selected bond distances and angles for **10** and **11** are given in Tables 3 and 4, while Tables 5 and 6 report non-hydrogen atomic coordinates and equivalent isotropic thermal parameters. The bond distances and angles, together with refinement of all ligand hydrogen atoms (x , y , z , U_{iso}) for both complexes, favor an uncharged guanidine ligand attached to the metal through the imino nitrogen in each case.

The cobalt complex **10** has Co–NH₃ distances ranging from 1.956(4) to 1.969(4) Å, typical of Co(III), with the guanidine

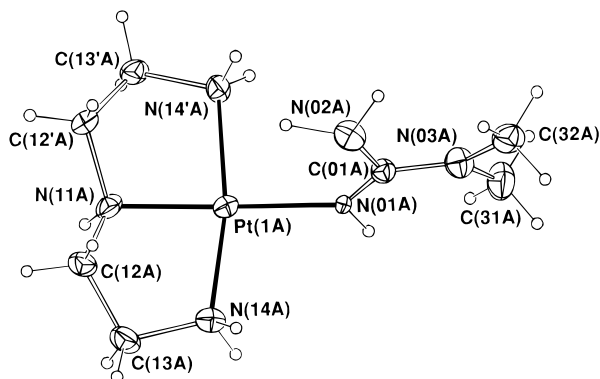


Figure 3. One cation (A) of **11**.

Table 3. Selected Non-Hydrogen Bond Lengths (Å) for Cations of **10** and **11** (A, B)^a

	10	11	
		11A	11B
Co–N(1)	1.964(3)	Pt–N(11)	1.984(6)
Co–N(2)	1.969(4)	Pt–N(14)	2.046(6)
Co–N(3)	1.956(4)	Pt–N(14')	2.036(6)
Co–N(4)	1.963(5)	Pt–N(01)	2.018(7)
Co–N(5)	1.961(3)	N(01)–C(01)	1.31(1)
Co–N(01)	1.940(3)	C(01)–N(02)	1.394(8)
N(01)–C(01)	1.308(5)	C(01)–N(03)	1.33(1)
C(01)–N(02)	1.355(5)	N(03)–C(31)	1.46(1)
C(01)–N(03)	1.338(4)	N(03)–C(32)	1.43(1)
N(03)–C(31)	1.442(7)		
N(03)–C(32)	1.462(7)		

^a Two cations (A and B) per asymmetric unit.

nitrogen at 1.940(3) Å opposite the longest Co–NH₃ bond. The Co–N(01)–C(01) angle is 136.5(2)°. The guanidine ligand has a shorter CoN–C bond (1.308(5) Å), indicative of a higher C=N bond order, than the other C–NH₂ (1.355(6) Å) and C–NMe₂ (1.337(4) Å) bond lengths where there is still partial double bond character, rather like amides. The dihedral angle between the equatorial plane, defined by N(01), N(3), N(2), N(4), and Co, and the skeletal plane of the guanidine ligand is 51°. This deviation is probably the result of steric interaction between protons of the axial ammine N(5) and guanidine N(02) ligands.

The cobalt atom lies 0.542(6) Å out of the CN₃ conjugated component of the ligand plane (χ^2 10.6).

For the platinum complex **11** there were two molecules per asymmetric unit, pseudosymmetrically related, with the geometries and stereochemistries of the two cations being very similar. Extensive data acquisition with full refinement of hydrogen atom parameters enabled all hydrogen atoms, including those of the guanidine ligand, to be located. The planar geometry (χ^2 204, 266; δ Pt, N(11, 14, 14', 01) 0.005(1), –0.013(7), –0.073(8), –0.072(8), –0.027(8); 0.005(1), –0.003(7), –0.079(7), –0.082(8), –0.019(8) Å) has N(01)PtN(11) forming an approximately linear ridge with N(14,14') depressed to either side.

The N₃C cores of the guanidine ligands of **11** are closely coplanar, with appreciable deviation of the platinum atoms (δ Pt 0.30(1), 0.44(1) Å) and terminal methyl carbons (δ C(31,32) –0.35(1), 0.27(1) Å; –0.38(1), 0.41(2) Å) indicating some twisting about the C(01)–N(03) bonds of the terminal CNMe₂ planes relative to the NCN₂ planes. The PtN₄/NCN₂ interplanar dihedral angles are 72.9(3) and 76.3(3)°. The dien ligands coordinate with their characteristic quasi-*m* symmetry; perturbations from this symmetry are found most notably (Table 7) with respect to the torsions about C(13)–N(14) and their primed equivalents. These differences may be associated with the deviation of the guanidine ligand from normality *vis-a-vis* the “plane” about the platinum atom. This may be caused by the dien NH hydrogen atoms being more intimately involved, than the NH hydrogen of the guanidine ligand, in hydrogen bonding with the anion oxygen atoms (Table 8). The distances from the platinum atoms to the central nitrogens for the dien ligands are shorter than the distances to the peripheral nitrogens, an effect of the guanidine ligand and/or the size of the metal atom being incompatible with linear N(14)–Pt–N(14') arrays.

For the guanidine ligand, the Pt–N–C angles (125.4(4), 127.9(5)°) are smaller than those in the Tc complex **6**⁴ but similar to values reported for the Pt–canavine dimer (122–130°).² Within the dimethylguanidine ligands themselves, torsions about the central C–N bonds are appreciable (N₂CN/CNC₂ dihedral angles 14.4(4), 18.6(4)°) and the heavy atom reduces the precision of the structural data. Nonetheless the geometries are consistent with appreciable delocalization of the imino double bonds among the possible sites. Although

Table 4. Selected Non-Hydrogen Bond Angles (deg) for Cations of **10** and **11** (A, B)^a

	10	11 ^a	
		11A	11B
N(1)–Co–N(2)	89.6(1)	N(11)–Pt–N(14)	84.4(2)
N(1)–Co–N(3)	87.8(2)	N(11)–Pt–N(14')	84.6(2)
N(1)–Co–N(4)	91.6(2)	N(11)–Pt–N(01)	178.6(2)
N(1)–Co–N(5)	178.1(2)	N(14)–Pt–N(14')	168.2(2)
N(1)–Co–N(01)	88.1(1)	N(14)–Pt–N(01)	95.3(3)
N(2)–Co–N(3)	89.9(2)	N(14')–Pt–N(01)	95.6(3)
N(2)–Co–N(4)	90.5(2)	Pt(1)–N(01)–C(01)	125.4(4)
N(2)–Co–N(5)	89.0(1)	N(01)–C(01)–N(02)	118.6(7)
N(2)–Co–N(01)	177.3(2)	N(01)–C(01)–N(03)	123.0(6)
N(3)–Co–N(4)	179.2(2)	N(02)–C(01)–N(03)	118.4(7)
N(3)–Co–N(5)	93.4(2)	C(01)–N(03)–C(31)	121.1(6)
N(3)–Co–N(01)	91.4(2)	C(01)–N(03)–C(32)	121.3(7)
N(4)–Co–N(5)	87.2(2)	C(31)–N(03)–C(32)	117.5(7)
N(4)–Co–N(01)	88.1(2)		
N(5)–Co–N(01)	93.3(1)		
Co–N(01)–C(01)	136.5(2)		
N(01)–C(01)–N(02)	120.1(3)		
N(01)–C(01)–N(03)	122.6(3)		
N(02)–C(01)–N(03)	117.3(3)		
C(01)–N(03)–C(31)	121.3(4)		
C(01)–N(03)–C(32)	122.9(4)		
C(31)–N(03)–C(32)	115.1(4)		

^a Two molecules (A and B) per asymmetric unit.

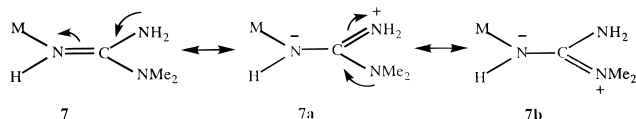
Table 5. Atomic Coordinates and Equivalent Isotropic Thermal Parameters (U , Å²) for Non-Hydrogen Atoms of **10**

atom	<i>x</i>	<i>y</i>	<i>z</i>	$U(\text{eq})$, Å ²
Co	0.18420(4)	0.68635(4)	0.67031(6)	0.0201(2)
N(1)	0.0244(3)	0.8194(3)	0.7124(5)	0.031(1)
N(2)	0.1090(4)	0.5661(3)	0.8334(5)	0.035(1)
N(3)	0.2221(3)	0.7596(3)	0.8595(4)	0.030(1)
N(4)	0.1450(4)	0.6152(4)	0.4795(5)	0.034(1)
N(5)	0.3410(3)	0.5491(3)	0.6281(5)	0.028(1)
N(01)	0.2508(3)	0.8084(3)	0.5069(4)	0.027(1)
C(01)	0.3603(3)	0.8251(3)	0.4376(4)	0.026(1)
N(02)	0.4551(3)	0.7745(4)	0.5162(5)	0.042(1)
N(03)	0.3850(3)	0.8877(3)	0.2865(4)	0.031(1)
C(31)	0.2955(5)	0.9278(6)	0.1812(7)	0.052(2)
C(32)	0.4937(4)	0.9387(6)	0.2299(7)	0.050(2)
S(1)	0.07235(9)	1.15498(9)	0.7586(1)	0.0324(3)
S(2)	0.20238(8)	1.23938(9)	0.5868(1)	0.0340(3)
S(3)	0.43736(8)	0.4575(1)	0.0910(1)	0.0328(3)
O(11)	0.0151(3)	1.1052(3)	0.6462(4)	0.044(1)
O(12)	0.1398(3)	1.0554(3)	0.8579(4)	0.062(2)
O(13)	-0.0109(3)	1.2657(3)	0.8560(4)	0.057(1)
O(21)	0.2548(3)	1.3002(3)	0.6951(4)	0.053(1)
O(22)	0.1286(3)	1.3344(3)	0.4891(4)	0.057(1)
O(23)	0.2917(3)	1.1334(3)	0.4906(5)	0.069(1)
O(31)	0.5096(3)	0.3270(3)	0.1227(4)	0.056(1)
O(32)	0.4010(3)	0.5389(3)	0.2393(4)	0.063(1)
O(33)	0.3396(3)	0.4630(3)	0.0067(4)	0.055(1)
O(1)	-0.1692(3)	0.6971(4)	0.9036(5)	0.081(2)

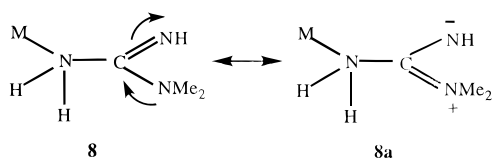
$$^a U_{\text{eq}} = 1/3 \sum_i \sum_j U_{ij} a_i^* a_j^* a_i a_j$$

deviations of the associated angles from the trigonal 120° are not large, N(01)–C(01)–N(03) angles are somewhat increased to ≥ 123° at C(01) and C(31)–N(03)–C(32) angles diminished to ≤ 118°. The platinum atoms lie 0.30(1) and 0.44(1) Å out of the ligand CN₃ skeletal planes.

Together with the short N–C bonds (Table 3), indicative of appreciable C=N bond order rather like that seen in amides, the bond angles suggest that double bond character is enhanced in C(01)–N(01) and diminished in C(01)–N(02) and C(01)–N(03). Structures **10** and **11** are therefore clearly consistent only with **7** whereas **8** (or **9**) requires a single MN–C bond as the electron lone pair on nitrogen is utilized in σ bonding to the metal. The stability of **7** is attributed to a conjugated array resulting from resonance stabilization (**7** ↔ **7a** ↔ **7b**)



which is less extensive in the alternative structures **8** (or **9**)

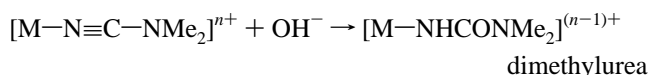
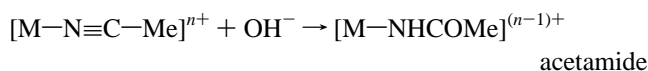


The M–N–C angles and N–C distances for guanidine in **10** and **11** are very similar to those reported⁴ for the Tc complex **6**. The M–N–C angle of **11** (131°) is slightly greater than that in the reported Pt–canavine dimer (122, 124, 127, 130°) where the bidentate bridging guanidine most likely imposes a steric constraint.² The structure of the osmium complex has not been determined, but the elemental analyses are consistent with the cation [(NH₃)₅OsNH=C(NH₂)NMe₂]³⁺. This structure is preferred to alternative tautomers **8** and **9** for the same reasons described above. Also the susceptibility of the osmium-

coordinated cyanamide ligand to hydration (see ahead) is almost identical to that of the other metalated cyanamides and therefore we expected amination to be similar, forming **7**.

Hydration of Nitriles. We measured the rate of absorbance change in aqueous NaOH (0.1–0.5 M) for [(NH₃)₅OsNCNMe₂]³⁺ and, for comparison, a [(NH₃)₅CoNCMe]³⁺ standard which has been measured before.^{16a} In later work we used a conventional spectrophotometer to measure the hydration of [dienPtNCNMe₂]²⁺ vs [(NH₃)₅CoNCNMe₂]³⁺, but these measurements were necessarily limited to low [OH⁻] because of the speed of hydration. The data are recorded in Table 9.

It was established by elemental analyses and NMR (¹H, ¹³C) spectra for the isolated products of these base hydrolyses reactions that nucleophilic attack by hydroxide on coordinated acetonitrile^{13,16a} or dimethylcyanamide^{8b,e} ligands gave exclusively coordinated acetamide or dimethylurea respectively:



The protonated forms of the Pt and Co products (pK_a 2–6) have now been unequivocally established as [dienPtNH₂CONMe₂]²⁺,^{8e,18} [dienPtNH=C(OH)Me]²⁺,¹³ [(NH₃)₅CoNH₂CONR₂]³⁺,^{8a} and [NH₃)₅CoNH=C(OH)Me]³⁺.^{17a}

For [(NH₃)₅CoN≡C–Me](CF₃SO₃)₃, [(NH₃)₅OsN≡C–NMe₂](BF₄)₃, [dienPtN≡C–NMe₂](CF₃SO₃)₂, and [(NH₃)₅CoN≡C–NMe₂](CF₃SO₃)₃, respectively, the base-catalyzed hydration experiments (Table 9) gave plots of k_{obs} vs [OH⁻] that were strictly linear (Figures 4 and 5), obeying the simple rate law

$$\text{rate} = k[\text{OH}^-][\text{complex}] \quad k_{\text{obs}} = k[\text{OH}^-]$$

under conditions where [OH⁻] was ≥ 10 × [Pt], [Co], or [Os]. Thus only a first order dependence on [OH⁻] was observed for all four complexes. The magnitude of k_{OH} did not differ much between the different complexes (Table 9).

These results contrast with those reported¹⁰ for [(NH₃)₅CoN≡CMe]³⁺, [(NH₃)₅RhN≡CMe]³⁺, and [(NH₃)₅IrN≡CMe]³⁺ where pronounced curvature was detected in plots of k_{obs} vs [OH⁻] in the concentration range 0.1–0.4 M [OH⁻]. However in the present work we could not detect any such curvature (even for Co(III)) for the similar range 0.05–0.5 M [OH⁻]. We were unable to examine this reaction at higher [OH⁻] where the reactions were too fast to measure with our conventional techniques. Unlike the 3d metal Co^{III}, the 5d metal Os^{III} is known to possess some π-basicity⁶ so some d-orbital effect may be possible¹⁰ but was not found here.

Enhancements in nitrile electrophilicity of up to ×10⁹ have been reported in the base hydrolysis of acetonitrile complexes of (NH₃)₅M^{III} ions.^{15,16,19} π-Back-bonding through interaction of metal dπ orbitals with the nitrile pπ orbital can offset the electrophilic induction, as evidenced for the π-donor Ru^{II}, which provides negligible electrophilic activation of acetonitrile^{6,15} (Table 10). This deactivation might also be expected for heavy

(18) Fairlie, D. P.; Woon, T. C.; Wickramasinghe, W. A.; Willis, A. C. *Inorg. Chem.* **1994**, *33*, 6425.

(19) Metal activation of other nitriles (a) Breslow, R.; Fairweather, R.; Keana, J. *J. Am. Chem. Soc.* **1967**, *89*, 2135. (b) Bennett, M. A.; Yoshida, T. *J. Am. Chem. Soc.* **1973**, *95*, 3030. (c) Diamond, S. E.; Grant, B.; Tom, G. M.; Taube, H. *Tetrahedron Lett.* **1974**, *46*, 4025. (d) Jensen, C. M.; Troglor, W. C. *J. Am. Chem. Soc.* **1986**, *108*, 723. (e) Ellis, W. R., Jr.; Purcell, W. L. *Inorg. Chem.* **1990**, *29*, 140. (f) Kim, J. H.; Britten, J.; Chin, J. *J. Am. Chem. Soc.* **1993**, *115*, 3618.

Table 6. Atomic Coordinates and Equivalent Isotropic Thermal Parameters (U , Å²) for Non-Hydrogen Atoms in **11**, [dienPtNH=C(NH₂)NMe₂](CF₃SO₃)₂

atom	(molecule A)				(molecule B)			
	x	y	z	$U(\text{eq}),^a$ Å ²	x	y	z	$U(\text{eq}),^a$ Å ²
Pt(1)	0.53857(2)	0.42800(2)	0.71743(1)	0.03709(9)	0.95641(2)	0.66108(2)	0.27763(1)	0.03472(8)
N(11)	0.5568(4)	0.4799(3)	0.6383(3)	0.043(2)	0.9387(4)	0.7174(3)	0.3560(3)	0.039(2)
C(12)	0.5399(6)	0.4048(5)	0.5916(4)	0.059(3)	0.9591(5)	0.6450(5)	0.4048(3)	0.052(3)
C(13)	0.6007(6)	0.3249(5)	0.6229(4)	0.059(3)	0.8981(6)	0.5640(5)	0.3757(4)	0.058(3)
N(14)	0.5820(4)	0.3091(4)	0.6849(3)	0.049(2)	0.9189(4)	0.5431(4)	0.3148(3)	0.043(2)
C(12')	0.4928(6)	0.5626(5)	0.6219(4)	0.059(3)	1.0020(6)	0.8001(5)	0.3691(4)	0.054(3)
C(13')	0.5079(6)	0.6157(5)	0.6826(4)	0.054(3)	0.9828(6)	0.8505(5)	0.3072(4)	0.057(3)
N(14')	0.4883(4)	0.5541(4)	0.7310(3)	0.051(2)	1.0026(4)	0.7869(4)	0.2590(3)	0.044(2)
N(01)	0.5168(4)	0.3740(4)	0.7967(3)	0.051(2)	0.9765(4)	0.6046(4)	0.1997(3)	0.049(2)
C(01)	0.4299(5)	0.3626(4)	0.8084(3)	0.044(3)	1.0597(5)	0.5951(5)	0.1839(3)	0.046(3)
N(02)	0.3435(4)	0.3776(5)	0.7601(3)	0.061(3)	1.1483(5)	0.6041(5)	0.2290(3)	0.068(3)
N(03)	0.4202(5)	0.3407(4)	0.8647(3)	0.059(3)	1.0640(5)	0.5763(4)	0.1253(3)	0.063(3)
C(31)	0.3256(7)	0.3068(6)	0.8727(5)	0.077(4)	1.1533(8)	0.5408(6)	0.1117(5)	0.087(5)
C(32)	0.5039(7)	0.3428(7)	0.9189(4)	0.085(4)	0.9769(8)	0.5932(7)	0.0724(4)	0.095(5)
S(1)	0.2727(1)	0.5953(1)	0.83764(8)	0.0439(6)	0.7777(1)	0.3216(1)	0.34534(9)	0.0477(7)
O(11)	0.2140(4)	0.5168(3)	0.8129(2)	0.059(2)	0.7147(4)	0.2446(3)	0.3223(3)	0.064(2)
O(12)	0.2213(4)	0.6808(3)	0.8231(2)	0.060(2)	0.7306(4)	0.4082(4)	0.3299(3)	0.066(2)
O(13)	0.3730(4)	0.5957(4)	0.8320(3)	0.064(2)	0.8768(4)	0.3170(4)	0.3385(3)	0.078(3)
C(11)	0.2878(6)	0.5845(5)	0.9214(4)	0.059(3)	0.7954(6)	0.3138(6)	0.4298(4)	0.065(3)
F(11)	0.3400(5)	0.5122(4)	0.9451(3)	0.111(3)	0.8518(5)	0.3804(4)	0.4594(2)	0.106(3)
F(12)	0.3307(5)	0.6545(4)	0.9531(2)	0.104(3)	0.7090(4)	0.3195(5)	0.4443(3)	0.114(3)
F(13)	0.1999(4)	0.5755(4)	0.9339(3)	0.107(3)	0.8388(5)	0.2394(4)	0.4538(3)	0.115(3)
S(2)	0.3182(1)	0.2085(1)	0.63585(9)	0.0489(7)	0.1854(1)	0.4527(1)	0.3732(1)	0.0498(7)
O(21)	0.4138(4)	0.1891(4)	0.6773(3)	0.068(2)	0.1878(5)	0.5491(4)	0.3781(3)	0.079(3)
O(22)	0.3047(5)	0.3009(4)	0.6171(3)	0.086(3)	0.0927(4)	0.4181(4)	0.3396(3)	0.082(3)
O(23)	0.2366(4)	0.1684(4)	0.6528(3)	0.087(3)	0.2697(4)	0.4130(4)	0.3586(3)	0.092(3)
C(21)	0.3233(7)	0.1493(7)	0.5666(5)	0.085(4)	0.1983(8)	0.4174(7)	0.4520(5)	0.096(5)
F(21)	0.3420(5)	0.0625(4)	0.5778(3)	0.115(3)	0.1226(6)	0.4488(5)	0.4721(3)	0.154(4)
F(22)	0.2396(5)	0.1525(5)	0.5238(3)	0.143(4)	0.1942(7)	0.3278(4)	0.4554(4)	0.160(5)
F(23)	0.3934(5)	0.1814(5)	0.5425(3)	0.142(4)	0.2792(7)	0.4445(7)	0.4892(4)	0.219(6)

$$^a U_{\text{eq}} = \frac{1}{3} \sum_i \sum_j U_{ij} a_i^* a_j^* a_{ij}$$

Table 7. Dien Ligand Torsion Angles (deg)^a for **11**

atoms	cation A	cation B
Pt–N(11)–C(12)–C(13)	–48.4(7), 44.8(6)	–49.5(6), 46.4(6)
N(11)–C(12)–C(13)–N(14)	49.0(8), –53.1(8)	52.2(7), –54.7(7)
C(12)–C(13)–N(14)–Pt	–25.8(6), 36.0(6)	–29.2(6), 36.2(6)
N(14)–Pt–N(01)–C(01)	–110.0(6), 65.5(6)	–111.9(6), 63.1(6)

^a Two values in each entry are for unprimed and primed ligand sections respectively.

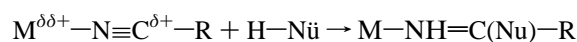
Table 8. Ligand Hydrogen···Anion Contacts, H···O ≤ 2.5 Å^a, for **11**

Cation A		Cation B	
atoms	contact	atoms	contact
Guanidine Ligand			
H(01)···O(11 ⁱ)	2.31(1)	(H(01)···O(11 ⁱⁱ))	2.59(6)
H(02a)···O(22)	2.49(6)	(H(02a)···O(21))	2.60(8)
H(02b)···O(11)	2.32(7)	H(02b)···O(11)	2.28(7)
Dien Ligand			
H(11)···O(23 ⁱⁱ)	2.15(5)	H(11)···O(23 ⁱⁱ)	2.14(5)
H(14a)···O(21)	1.86(6)	H(14a)···O(11 ⁱⁱ)	2.13(6)
H(14b)···O(11 ⁱⁱ)	2.35(6)	H(14b)···O(22 ^v)	2.10(5)
H(14a')···O(21 ^{iv})	2.23(5)	H(14a')···O(12 ^{vi})	2.25(5)
H(14b')···O(12 ⁱⁱ)	2.30(5)	H(14b')···O(22)	2.20(5)

^a Contacts are mainly between the ligand and anion of the same label (i.e. A···A, B···B); where the anion atom is of the other type, it is italicized. Transformations of the asymmetric unit: (i) $x, \frac{1}{2} - y, \frac{1}{2} + z$; (ii) $1 - x, 1 - y, 1 - z$; (iii) $1 - x, \frac{1}{2} + y, 1 \frac{1}{2} - z$; (iv) $1 + x, y, z$; (v) $1 - x, 1 \frac{1}{2} + y, z - \frac{1}{2}$; (vi) $1 - x, \frac{1}{2} + y, \frac{1}{2} - z$.

third row transition metals which have radially extended M $d\pi$ orbitals that permit greater π overlap with the weak π -accepting nitrile. However neither the weak π -donor⁶ Os(NH₃)₅³⁺ nor Pt(dien)²⁺ show different activation enhancements (both ca. 10⁶ fold) from first and second row transition metals (Table 10).

Final Comments. The metal-induced enhancement in electrophilicity of nitriles has been further demonstrated here by the reactivity of a cyanamide, bonded either by soft or hard metal electrophiles, toward nucleophilic attack by either ammonia or hydroxide:



Acetonitrile has previously been converted to acetamidine on Pt^{II} and Co^{III} by reaction with ammonia.²⁰ Whether amines similarly act as effective nucleophiles on nitriles in biological environments remains to be determined, but in principle the amine side chain of ornithine for example could attack a metal-bound cyanamide to give arginine if (i) the amine is correctly positioned, (ii) it is not protonated, and (iii) the bound cyanamide is not deprotonated²¹—all these factors may be possible in a hydrophobic protein environment.

Some interesting comparisons can be made between stabilities of metal complexes of tautomeric forms of guanidine, amide, and urea ligands. Tautomers **7** and **8** are isoelectronic with the urea complexes **12** and **13** respectively. For both the hard (NH₃)₅Co^{III} moiety and the softer dienPt^{II}, **12** is kinetically preferred over **13**,^{8a,e} just as **7** is preferred over **8**. On the other hand, while **12** is also thermodynamically preferred by (NH₃)₅-Co^{III}, **13** is thermodynamically more stable for dienPt^{II}.^{8a,e} Undoubtedly the preference for the imino tautomers **7** and **12** is related to the resonance stabilization that comes from π -electron density being delocalised over all four guanidine/

(20) (a) Stephenson, N. C. *J. Inorg. Nucl. Chem.* **1962**, *24*, 801. (b) Fairlie, D. P.; Jackson, W. G. *Inorg. Chem.* **1990**, *29*, 140.

(21) Balahura, R. J.; Jordan, R. B. *J. Am. Chem. Soc.* **1971**, *93*, 625.

(22) (a) For CN⁻, see ref 16b. (b) For azide, see: Ellis, W. R., Jr.; Purcell, W. L. *Inorg. Chem.* **1982**, *21*, 834. (c) For CO₃²⁻, see ref 16c.

Table 9. Metal Activation of Nitriles: Rates of Base Hydrolysis of Nitrile Complexes of Co^{III}, Os^{III}, and Pt^{II} ^a

[OH ⁻], M	[(NH ₃) ₅ CoNCMe](CF ₃ SO ₃) ₃ ^b <i>k</i> _{obs} , s ⁻¹ (<i>k</i> _{OH} , M ⁻¹ s ⁻¹)	[(NH ₃) ₅ OsNCNMe ₂](BF ₄) ₃ ^b <i>k</i> _{obs} , s ⁻¹ (<i>k</i> _{OH} , M ⁻¹ s ⁻¹)
0.05	0.213 (4.2)	0.261 (5.2)
0.10	0.398 (4.0)	0.435 (4.4)
0.20	0.708 (3.5)	0.791 (4.0)
0.30	1.203 (4.0)	1.306 (4.4)
0.40	1.601 (4.0)	1.884 (4.7)
0.50	2.147 (4.3)	2.330 (4.7)
av <i>k</i> _{OH} [complex], M	(4.0) [Co] = 2.9 × 10 ⁻⁴	(4.5) [Os] = 2.9 × 10 ⁻⁴ M

[OH ⁻], M	[(NH ₃) ₅ CoNCNMe ₂](CF ₃ SO ₃) ₃ ^c <i>k</i> _{obs} , s ⁻¹ (<i>k</i> _{OH} , M ⁻¹ s ⁻¹) ^c	[dienPtNCNMe ₂](CF ₃ SO ₃) ₂ ^c <i>k</i> _{obs} , s ⁻¹ (<i>k</i> _{OH} , M ⁻¹ s ⁻¹)
× 10 ²	× 10 ²	× 10 ²
2.60	—	7.52 (2.9)
1.96	—	5.47 (2.8)
1.31 ₆	3.08 ₆ (2.3)	—
0.66 ₂	1.51 (2.3)	1.98 (3.0)
0.16 ₄	0.38 (2.3)	0.48 ₃ (2.9)
av <i>k</i> _{OH} [complex], M	(2.3) [Co] = 1.3 × 10 ⁻⁴ M	(2.9) [Pt] = 1.03 × 10 ⁻⁴ M

^a T = 298 K; I = 1.0 M (NaClO₄). ^b Stopped-flow. ^c Conventional spectroscopy.

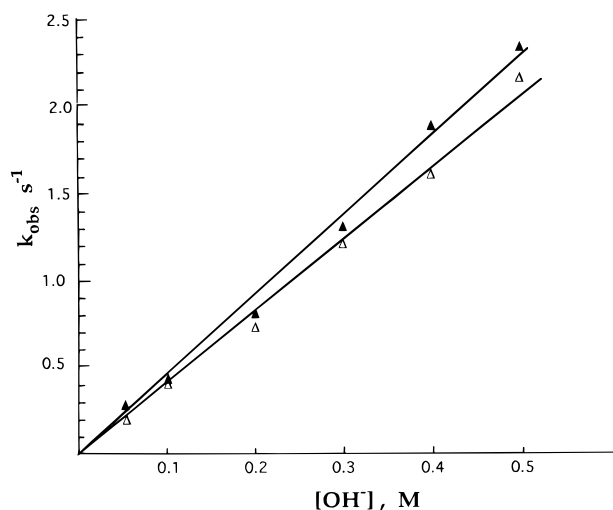
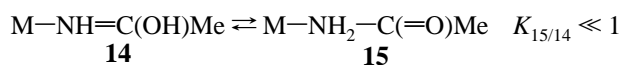
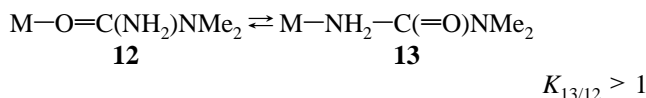
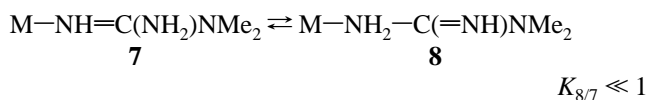


Figure 4. Plots of *k*_{obs} vs [OH⁻] for absorbance changes of [(NH₃)₅CoN≡CMe](CF₃SO₃)₃ (Δ) and [(NH₃)₅OsN≡CNMe₂](BF₄)₃ (▲) at 240 and 300 nm respectively (298 K; I = 1.0 M NaClO₄; [Os] = [Co] = 2.9 × 10⁻⁴ M).

urea non-hydrogen atoms, whereas there can be no double bond character in the MNH₂-C bond for **8** and **13**.



A further analogy is drawn between the guanidine tautomers and the isoelectronic amide ligand (e.g. R = Me), where the iminol form **14** (cf. **7**) is more stable than the (unknown) amide form **15** (cf. **8**) when bound through nitrogen to metal ions, including dienPt^{II} or (NH₃)₅Co^{III}.^{13,17,18}

The method we have used to prepare coordination complexes of a guanidine and urea may also have biological relevance.

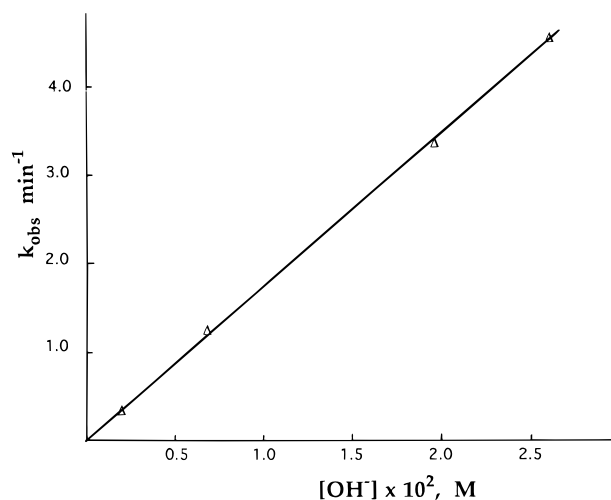


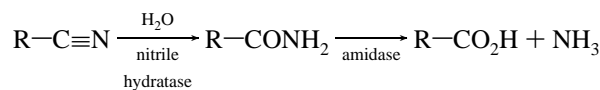
Figure 5. Plot of *k*_{obs} vs [OH⁻] for absorbance changes of [dienPtN≡CNMe₂](CF₃SO₃)₂ at 236 nm (298 K; I = 1.0 M NaClO₄; [Pt] = 1.03 × 10⁻⁴ M).

Table 10. Metal-Activation of Nitriles: Comparison of Rates of Base Hydrolyses of Metal-Nitrile Complexes

	<i>k</i> _{OH} , M ⁻¹ s ⁻¹ (298 K)
N≡CMe	1.6 × 10 ⁻⁶ ^a
[(NH ₃) ₅ RuN≡CMe](BF ₄) ₂	6 × 10 ⁻⁵ ^a
[(NH ₃) ₅ RhN≡CMe](ClO ₄) ₃	1.0 ^a
[(NH ₃) ₅ CoN≡CMe](ClO ₄) ₃	3.4; ^b 4.0 ^c
[(NH ₃) ₅ RuN≡CMe](ClO ₄) ₃	2.2 × 10 ² ^a
[(dien)PtN≡CNMe ₂](CF ₃ SO ₃) ₂	2.9 ^c
[(NH ₃) ₅ CoN≡CNMe ₂](CF ₃ SO ₃) ₃	3.0; ^d 2.3; ^c 2.1 ^e
[(NH ₃) ₅ OsN≡CNMe ₂](BF ₄) ₃	4.5 ^c

^a Reference 15a. ^b Reference 16a. ^c This work, I = 1.0 M (NaClO₄). ^d Reference 8b, I = 1.0 M KCl. ^e Fairlie, D. P. Ph.D. dissertation, University of NSW, 1983. I = 1.0 M (NaClO₄), T = 298 K, NEt₃/NEt₃H⁺ buffers; *k*_{OH} = 2.5 M⁻¹ s⁻¹, 0.5 M (LiClO₄), T = 298 K, NEt₃/NEt₃H⁺ buffers.

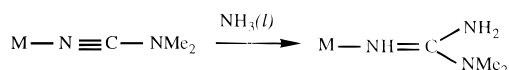
Microorganisms are known to convert nitriles into carboxylic acids using nitrilases.⁷



Many bacteria do this via two enzymes, a nitrile hydratase that

catalyzes hydration of nitriles to amides followed by an amidase that deaminates the amide to an acid. Nitrile hydratase has a low-spin non-heme Fe^{III} which binds directly to aliphatic nitriles and mediates their enzymatic hydration in bacteria.⁷ This is mimicked by numerous electrophilic metals which similarly activate nitriles ($\leq 10^9$ -fold; Table 10) to attack by nucleophiles like OH⁻, H₂O, CN⁻, N₃⁻, CO₃²⁻.²² Jack bean urease uses Ni^{II} to carry out the second stage (R = NH₂), hydrolysis⁹ of urea to carbamate and ammonia.

The electrophilicity enhancement demonstrated here by activation of a cyanamide, bonded either by hard or soft metals, has now been utilized in the nucleophilic attack by ammonia on the cyanamide ligand to produce a guanidine ligand:



This newly recognized coordinating ability of guanidines, irrespective of the hard/soft character of the metal, may be relevant in hydrophobic biological environments where electrophilic metal ions may compete better with the proton. However there is currently no known biological precedent for metal-assisted amination of nitriles by amines.

Experimental Section

A Beckmann Acta MVII 5270 spectrophotometer was used to measure absorbances of the Os and Co complexes. An Aminco-Morrow stopped-flow apparatus and Beckmann DU spectrophotometer were used as described²³ to monitor base-catalyzed hydration of the Os and Co nitrile complexes. A Gemini 300 MHz Varian NMR spectrometer, Varian Cary 3 UV-vis, and Perkin-Elmer 1600-FT infrared spectrophotometers were used. Analyses of cobalt and osmium complexes were determined by Stanford University Microanalytical Services. Platinum complexes were analysed by Chemical & Microanalytical Services, North Essendon, Melbourne, Australia. All solvents were analytical grade.

Synthesis. [(NH₃)₅CoN≡CNMe₂](CF₃SO₃)₃,^{8b} [(NH₃)₅CoN≡CMe](CF₃SO₃)₃,^{16a} [(NH₃)₅Os(OsSCF₃)](CF₃SO₃)₂¹² were prepared as described. Some properties of [(NH₃)₅CoNHCONMe₂](CF₃SO₃)₂^{8b} and [dienPtNHCONMe₂](CF₃SO₃)₂^{8b} have been described elsewhere, those of [(NH₃)₅OsNH=C(NH₂)NMe₂](CF₃SO₃)₃ and [(NH₃)₅OsNHCO-NMe₂](CF₃SO₃)₂ will be reported^{8f} in studies of a wide range of new pentaammineosmium(III) complexes.

[DienPtOH₂](CF₃SO₃)₂. K₂PtCl₄ (10 g) was dissolved in water (60 mL) and reacted with KI in water (16 g in 10 mL). After warming (10 min, 40 °C), diethylenetriamine (2.5 g) was added dropwise to the stirred dark brown solution. The resulting brown precipitate of [dienPtI₂] was filtered and washed thoroughly with ethanol and diethyl ether before drying under vacuum at 40 °C. Isolated yield = 11.0 g. This was suspended in water (100 mL) and stirred with AgCF₃SO₃ (10.2 g in 10 mL water) in the dark for 18 h at 50 °C. The AgI precipitate was removed by filtration (filter aid), and the filtrate was evaporated under vacuum at 45 °C. The white solid residue was washed (diethyl ether, 3 × 100 mL), recrystallized (ethanol/ether) and dried under vacuum. Yield: 7.4 g. Anal. Calcd: C, 11.72; H, 2.44; N, 6.84; S, 10.42. Found: C, 11.63; H, 2.46; N, 6.92; S, 10.49. ¹H-NMR, δ (acetone-*d*₆, TMS): 7.35 (2H, H₂O); 6.99, 6.80 (1H, NH); 5.56, 5.42 (4H, NH₂); 2.7–3.3 (8H, CH₂). ¹³C-NMR, δ (acetone-*d*₆, TMS): 56.4, 51.2, 50.9 (dien).²⁴

[DienPtN≡CNMe₂](CF₃SO₃)₂. [DienPtOH₂](CF₃SO₃)₂ (1.6 g) was dissolved in 1,1-dimethylcyanamide (3 mL) and stirred for 45 min at 22 °C in a stoppered flask. The reaction mixture was washed by decantation with diethyl ether (3 × 10 mL) to remove traces of dimethylcyanamide. The oily residue was dried by vacuum evaporation and redissolved in acetone (3 mL) to which diethyl ether (0.5 mL)

was added dropwise. After this was allowed to stand for 2 h at room temperature, transparent (hygroscopic) crystals were collected by filtration and washed (CH₂Cl₂, ether). Isolated yield: 1.5 g. Anal. Calcd: C, 16.21; H, 2.85; N, 10.50; S, 9.60. Found: C, 15.99; H, 2.85; N, 10.64; S, 9.40. ¹³C-NMR, δ (acetone-*d*₆, TMS) 120.7 (N≡C), 128.3, 124.1, 119.8, 115.6 (CF₃), 55.7, 51.4 (dien), 39.8 (NMe₂). IR spectrum. ν (cm⁻¹, Nujol) 3235, 3141 (br, NH); 2297 (Pt–N≡CNMe₂). Free N≡CNMe₂, 2215 cm⁻¹.

[DienPtN≡CMe](CF₃SO₃)₂. [DienPtOH₂](CF₃SO₃)₂ (0.4 g) was dissolved in acetonitrile (4 mL) and stirred for 20 min at 22 °C in a stoppered flask. The reaction mixture was poured into diethyl ether (20 mL), and the residue was washed with more ether to remove residual nitrile before vacuum evaporation, dissolution in acetone (3 mL), and dropwise addition of diethyl ether. After 5 h at room temperature, transparent crystals were collected by filtration and washed (CH₂Cl₂, ether). Isolated yield: 0.35 g. Anal. Calcd: C, 15.1; H, 2.5; N, 8.8; S, 10.0. Found: C, 15.0; H, 2.65; N, 8.5; S, 9.8. ¹³C-NMR, δ (acetone-*d*₆, TMS) 121.5 (N≡C), 128.3, 124.1, 119.8, 115.6 (CF₃), 55.3, 51.2 (dien), 3.1 (Me).

[(NH₃)₅OsN≡CNMe₂](CF₃SO₃)₃. *N,N*-Dimethylcyanamide (30 mL) was added to [(NH₃)₅Os(CF₃SO₃)](CF₃SO₃)₂ (2 g), and the mixture was stirred at 40 °C for 15 min before cooling to room temperature and pouring into diethyl ether (100 mL). A brown precipitate was collected by filtration, washed with diethyl ether, and crystallized by dissolving it in cold water and filtering into 20% aqueous HBF₄. After cooling (0 °C, 45 min), the crystals were collected by vacuum filtration and washed (ethanol, ether) and then recrystallized by redissolving in water (50 mL) and adding filtered concentrated HBF₄ (20 mL). Anal. Calcd for [(NH₃)₅OsN≡CNMe₂](BF₄)₃: C, 5.95; H, 3.47; N, 16.19. Found: C, 6.27; H, 3.28; N, 16.10. Near-infrared: 2130 nm, medium intensity $\epsilon \sim 10^2 \text{ M}^{-1} \text{ cm}^{-1}$. IR: 2250 cm⁻¹ (C≡N). UV: λ_{max} 352 nm, ϵ 1573 M⁻¹ cm⁻¹.

[(NH₃)₅OsN≡CMe](CF₃SO₃)₂. Acetonitrile (10 mL) was degassed (two freeze–thaw cycles) before transferring under argon to an evacuated Schlenk tube containing 0.3 g [Os(NH₃)₅(OSO₂CF₃)](CF₃SO₃)₂ and filed Mg pieces. The mixture was stirred for 1 h under argon before filtering it through a fine Schlenk filter stick. The acetonitrile was evaporated to a few milliliters of a yellow solution and hexane was diffused slowly under argon into the solution. After 12 h, a pale crystalline solid had precipitated. This was collected and dried under vacuum. Anal. Calcd for [(NH₃)₅OsN≡CMe](CF₃SO₃)₂: C, 7.8; H, 2.9; N, 13.7; S, 10.4; F, 18.6. Found: C, 7.72; H, 3.05; N, 13.58; S, 10.2; F, 18.2. IR: 2200 cm⁻¹ (C≡N). The Os(III) analogue was similarly isolated without treatment with Mg. Anal. Calcd for [(NH₃)₅OsN≡CMe](CF₃SO₃)₃: C, 7.8; H, 2.4; N, 11.0; S, 12.6. Found: C, 7.7; H, 2.4; N, 10.8; S, 12.1. Near-IR: 2100 nm, $\epsilon \sim 10^2 \text{ M}^{-1} \text{ cm}^{-1}$. IR: 2300 cm⁻¹ (C≡N).

[(NH₃)₅CoNH=C(NH₂)NMe₂]₂(S₂O₆)₃·2H₂O. [(NH₃)₅CoN≡CNMe₂](CF₃SO₃)₃ was dissolved in NH₃(l) and left to react for 30 min before evaporating the solvent and crystallizing from aqueous 0.1 M Tris (pH 10.2). Recrystallization from aqueous Na₂S₂O₆ gave the dithionate salt; NaClO₄ gave the ClO₄⁻ salt. This compound chromatographed as a typical 3+ ion on Dowex 50W-x2 cation exchange resin (pH 0–10), not a 2+ ion.^{20b} Anal. Calcd for C₂₀N₁₆-C₆S₆H₄₈O₁₈: C, 7.36; H, 5.35; N, 22.89; S, 19.65. Found: C, 7.6; H, 5.1; N, 22.7; S, 18.9. ¹H-NMR, δ (DMSO-*d*₆, TMS): 2.60 (1H, CoNH=), 2.92 (6H, NMe₂), 3.13 (2H, H₂O), 3.34 (3H, *trans*-NH₃), 3.36 (12H, *cis*-NH₃), 5.74 (2H, NH₂). ¹³C-NMR, δ (DMSO-*d*₆, TMS): 162.2 (=C), 38.5 (NMe₂).

[DienPtNH=C(NH₂)NMe₂](CF₃SO₃)₂. [DienPtN≡CNMe₂](CF₃SO₃)₂ was reacted with NH₃(l) and crystallized as above. Anal. Calcd: C, 15.68; H, 3.19; N, 12.22; S, 9.31. Found: C, 15.80; H, 3.21; N, 12.29; S, 9.36. ¹H-NMR, δ (acetone-*d*₆, TMS): 3.00 (14H, NMe₂ + dien-CH₂); 4.31 (1H, PtNH=C); 5.22, 5.33 (4H, dien-NH₂); 5.97 (2H, PtNH=CNH₂); 6.22 (1H, dien-NH). ¹³C-NMR, δ (acetone-*d*₆, TMS): 162.1 (=C), 54.9, 52.2 (dien), 38.7 (NMe₂), 115.8, 120.1, 124.4, 128.6 (CF₃).

Kinetic Studies. The Pt complex was monitored at 236 nm by dissolving solid complex in 1.0 M NaClO₄ equilibrated at 25.0 °C in a 1 cm cuvette inserted in a Cary 3 spectrophotometer. The solution (3.0 mL) was titrated with NaOH (0.010–0.080 mL; 0.1 and 1.0 M). The solution temperature was measured with a temperature probe (25.0 ± 0.1 °C), and the temperature of the cell block was regulated with a

(23) Brown, G. M.; Sutton, J. E.; Taube, H. *J. Am. Chem. Soc.* **1978**, *100*, 2767.

(24) See ref 13, footnote 21.

standard Peltier electrochemical device that efficiently controls heat exchange by solid phase conductance. Data were collected over $5t_{1/2}$ and the rate was strictly first order as determined by standard graphical plots.

Stock solutions were made up of $[(\text{NH}_3)_5\text{CoNCMe}](\text{ClO}_4)_3$ and $[(\text{NH}_3)_5\text{OsNCNMe}_2](\text{BF}_4)_3$ complexes ($[\text{Co}]$, $[\text{Os}] = 2.9 \times 10^{-4}$ M) and NaOH (0.01–2 M; $\mu = 2$ M NaClO₄), prepared from 1.00 M NaOH analytical concentrate (Baker) and freshly distilled water. Equal volumes of the solutions were placed into syringes of an Aminco-Morrow stopped-flow apparatus described elsewhere.²³ To monitor the reaction of the rapidly mixed solutions (240 nm, Co; 300 nm Os; 25.0 °C) a Beckman DU spectrophotometer was connected to a cathode ray oscilloscope and traces were recorded, photographed and kinetic data ($\geq 5t_{1/2}$) were read off the photographs²³ and processed as above.

X-ray Structure Determination. Unique room temperature diffractometer data sets were measured for both complexes. The structures were solved by the conventional Patterson heavy atom method, and refined by full-matrix least-squares methods after analytical absorption corrections. Anisotropic thermal parameters were refined for the non-hydrogen atoms and, despite difficulties encountered due to the super

lattice of the Pt structure and high anion thermal motion, the parameters (x , y , z , $U_{\text{iso}}\text{H}$) were also refined. Neutral atom complex scattering factors were employed, together with the XTAL 3.0 program system²⁵ implemented by S. R. Hall.

Acknowledgment. The work was supported in part by grants from the Australian Research Council, the National Science Foundation, and the National Institutes of Health.

Supporting Information Available: Tables 11–13 containing full lists of bond lengths and angles, fractional coordinates of hydrogen atoms, anisotropic thermal parameters of non-hydrogen atoms, and calculated hydrogen positions (9 pages). Ordering information is given on any current masthead page.

IC961138E

(25) Hall, S. R.; Stewart, J. M., Eds. *The XTAL 3.0 Reference Manual*; Universities of Western Australia and Maryland: Nedlands, Australia, and College Park, MD, 1990.